Modified Lignin Nanosphere Adsorbent for Lead and Copper Ions

Baoshan Xie,* Yi Hou, and Youming Li

Heavy metal ions in wastewater have negative effects on humans and the environment. In this paper, the adsorption of lead and copper ions by modified eucalyptus lignin nanosphere (ECLNPs) was studied. The spherical alkali-lignin particles had a diameter of 50 nm, abundant carboxyl groups of 0.66 mmol/g, and relatively high adsorption performance. The equilibrium adsorption capacities of Pb(II) and Cu(II) by ECLNPs were 126.0 mg/g and 54.4 mg/g, respectively. Both Pb(II) and Cu(II) adsorptive processes fitted a pseudo-second-order kinetics model. In the simultaneous adsorption process of Pb(II) and Cu(II), ECLNPs had higher adsorptive selectivity for Pb(II) than Cu(II), and there was a competitive adsorption process between Pb(II) and Cu(II). This resulted from the lower hydration heat of Pb(II) in water, which leads to easier separation from water ligands. ECLNPs also showed good recyclability, with 16.6% and 21.1% loss in Pb(II) and Cu(II) adsorption capacity, respectively, after three consecutive adsorption-desorption cycles, which provides a feasible technical direction for the utilization of biomass resources and the treatment of water contamination.

Keywords: Carboxyl modified lignin nanospheres; Heavy metal ions; Adsorption performance; Adsorption mechanism; Biomass resources; Adsorbent

Contact information: State Key Laboratory of Pulp and Paper Engineering, South China University of Technology, 510640 Guangzhou, China; National Engineering Research Center of Papermaking and Pollution Control, South China University of Technology, 510640 Guangzhou, China;
** Corresponding author: ceyhou@scut.edu.cn*

INTRODUCTION

Water pollution is a societal problem that accompanies urbanization. Industrial activities, such as petroleum and chemical production, leather manufacturing, and battery manufacturing, release a large amount of inorganic metal ions and organic dye into water. Heavy metal ions such as copper (Cu), lead (Pb), and chromium (Cr) are poisonous, non-biodegradable, and not easily removed (Şengil and Özacar 2008; Malek *et al*. 2016; Meena *et al*. 2016; Nonkumwong *et al*. 2016). Adsorption is commonly used to remove ions due to its relatively low cost, good performance, and good reusability. Although adsorbents such as activated carbon, carbon nanotubes, *etc*., have been commercialized, their high cost is the biggest factor limiting their application. This limitation has prompted research into new adsorbents with lower costs and better performance.

Lignin is a natural polymer, second in abundance to cellulose. It is also a byproduct from the pulp and paper industry (Zong *et al*. 2018). When lignin is removed from fibers in the course of kraft pulping, most of it is incinerated as a means to generate energy and to recover the pulping chemicals. This is a low-value usage of the lignin. Thus, the high-value utilization of lignin as an adsorbent has future potential. To absorb heavy metal ions, carboxylic functional groups are grafted to lignin. There are only a small number of

carboxyl groups found in native lignin, so it cannot be used as an adsorbent directly. However, sufficient oxygen-containing functional groups, such as hydroxyls, allow the possibility of obtaining various functional groups by chemical modification of the lignin. Carboxymethylation assisted with microwave (Yan and Li 2016; Li *et al*. 2018; Nguyen *et al*. 2019), a method to introduce carboxyl groups into lignin, works better than reaction under high temperature or high pressure. It greatly enhances carboxyl functional groups, resulting in a higher adsorption capacity of heavy metal ions (Li *et al*. 2018). Lignin nanosphere materials have a relatively large surface area based on their regular shape and small volume. They have better mass transfer behavior based on improved diffusing and dispersing characteristics (Ge *et al*. 2016). Moreover, lignin nanospheres, prepared using ionic liquid and antisolvent, reduce the water solubility of modified lignin (Liu *et al*. 2018) but increase the chelation between carboxyl groups and ions (Zhao *et al*. 2011).

In this study, the adsorption performance of carboxyl-modified alkali-lignin nanospheres (ECLNPs) was inspected to broaden the high-value utilization of lignin (Celik and Demirbas 2005; Nonkumwong *et al*. 2016). The adsorption performance of ECLNPs was investigated in the Pb(II) solution, Cu(II), solution and simultaneous solution.

EXPERIMENTAL

Materials

Eucalyptus alba alkali lignin (EAL) was extracted from the sulfate pulp and purified, based on the method described by Wang *et al*. (2011). Sodium monochloroacetate (≥ 98%) was purchased from Sigma-Aldrich (Beijing, China). Ionic liquids [EMIM][Ac] were synthesized based on a published method (Liu *et al*. 2018). Other reagents used in the experiment were analytical grade products.

Preparation of Modified Lignin Nanospheres

Modified eucalyptus lignin nanospheres (ECLNPs) were synthesized in two steps (Liu *et al*. 2019). First, carboxyl-modified EAL (ECAL) was prepared in an aqueous phase. In the second step, ECLNPs were obtained by adding anti-solvent in the ionic system.

Adsorption Experiments

The experiments were conducted in 150 mL conical flasks with 50 mL of lead (or copper) nitrate solution and ECLNPs. The mixtures were reacted in an air-bath orbital shaker with a shaking speed of 150 rpm for 3 h at 30 °C. The factors studied were the initial concentration of lead (or copper) nitrate solution from 25 to 200 ppm and contact time from 0 to 3 h. The optimum conditions were determined, and the performance of EAL and ECLNPs was studied under optimum conditions. The Pb(II) and Cu(II) adsorbed by ECLNPs in separate and simultaneous adsorption was tested. All adsorption experiments were operated two times to avoid any occasional mistakes. Adsorption capacity was calculated according to Eq.1,

$$Q_e(mg/g) = \frac{C_0 - C_e}{m} \times V \quad (1)$$

where Q_e (mg/g) is the adsorbing capacity, C_0 (mg/mL) and C_e (mg/mL) are the initial concentrations and the equalized concentrations of copper (or lead) nitrate solution, respectively, V (mL) is the volume of solution, and m (g) is the mass of ECLNPs.

Regeneration Experiment

To test the recyclability of ECLNPs, three desorption-reabsorption cycles were carried out for Pb(II) and Cu(II). Metal ion-loading ECLNPs were mixed with HNO_3 at pH 2 for 2 h before washing and drying. The regenerated ECLNPs were used to re-adsorb metal ions.

^{31}P-NMR Analysis

^{31}P-NMR was carried out using a Bruker AVANCE 600 NMR spectrometer (Karlsruhe, Germany) to measure the content of the carboxyl groups in lignin-based materials. Twenty-five milligrams of sample was dissolved in 500 μL of anhydrous pyridine and deuterated chloroform (1.6:1, v/v) under stirring. Next, 100 μL of cyclohexanol and chromium(III) acetylacetonate solution (10.85 mg/mL and 5 mg/mL, respectively, in anhydrous pyridine and deuterated chloroform 1.6:1, v/v) was added as an internal standard and relaxation reagent. Finally, the mixture was reacted with 100 μL of 2-chloro-1,3,2-dioxaphospholane (TMDP) for 10 min.

XPS Analysis

The nanospheres sample before and after adsorption of Pb(II) and Cu(II) ions were analyzed using XPS (D8 ADVANCE, Bruker). All binding energies were referenced to the neutral C1s peak at 284.6 eV to compensate for surface charging effects.

RESULTS AND DISCUSSION

Characterization

The morphology of ECLNPs is shown in Fig. 1, as observed by SEM. The ECLNPs were nearly spherical in shape with a slight aggregation. The mean diameter was approximately 50 nm. According to specific surface area theory, the spherical particle offers larger superficial area than the irregular one, which is beneficial to adsorption.

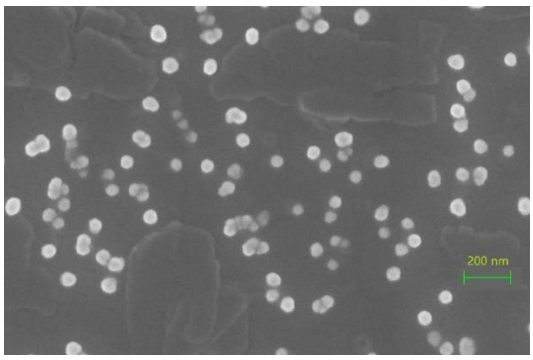

Fig. 1. SEM micrograph of ECLNPs

^{31}P-NMR analysis measures the content of the carboxyl groups in lignin-based materials (Granata and Argyropoulos 1995). The quantitative results of functional groups are tabulated in Table 1. The amount of carboxyl groups of ECLNPs was 0.66 mmol/g, almost 2 times that of the EAL (0.31 mmol/g), which means that the carboxyl group content increased after the experiment. The aliphatic hydroxyl group contents doubled. This result

might indicate that more aliphatic hydroxyl groups were exposed in loose lignin molecules after reaction with the sodium monochloroacetate (Li *et al*. 2018).

Table 1. The Contents of Functional Groups in EAL and ECLNPS

Adsorbents	Aliphatic OH (150-145.7 ppm)	Condensed phenolic OH (145-140.7 ppm)	Guaiacyl and catechol OH (140-137.6 ppm)	Total phenolic OH	Carboxyl (136-133.8 ppm)
	(mmol/g)	(mmol/g)	(mmol/g)	(mmol/g)	(mmol/g)
EAL	1.77	1.28	0.45	1.73	0.31
ECLNPs	2.95	1.29	0.57	1.86	0.66

Adsorption performance of EAL and ECLNPs

The adsorption performance between the original lignin and ECLNPs is shown in Fig. 2. The saturated adsorption capacity of Pb(II) for ECLNPs was 126.0 mg/g, which is almost ten times that of EAL (approximately 10 mg/g). The capacity of Cu(II) was 54.4 mg/g, five-fold higher than the original value. The adsorption performance was greatly enhanced after chemical modification, and the increase in carboxyl groups contents appeared to play an important role. The introduction of carboxyl groups to the lignin surface improved the hydrophilicity of lignin, and regular nanospheres provided a large specific surface. It is proposed that these changes were responsible for the increases in the maximum lead and copper uptake. The maximum adsorption capacity was higher than that of other adsorbents, as illustrated in Table 2, including polycarboxylic microspheres, modified cellulose, lignin microspheres, nanometer-sized ZrO_2.

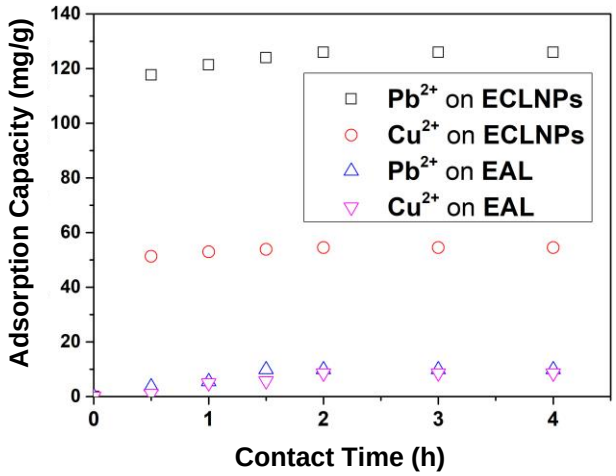

Fig. 2. The Pb(II) and Cu(II) absorbing capacity by EAL and ECLNPs

The XPS method has been used to analyze the metal-loaded ECLNPs and confirm the interaction mechanism. Figure 3 shows the XPS spectra of ECLNPs before and after Pb(II) and Cu(II) adsorption. The Pb4f peak (139.4 eV) and Cu2p peak (934.6 eV) were detected on the ECLNPs surface after adsorption, indicating that ECLNPs were successfully adsorbed Pb(II) and Cu(II).

Table 2. Comparison of Adsorption Capacity of Different Adsorbents Towards Pb(II) and Cu(II)

Ions	Adsorbents	Q_e (mg/g)	Ref.
Pb(II)	Polycarboxylic microspheres	20.1	Dakova *et al*. (2009)
	Modified cellulose	28.3	Aoki *et al*. (1999)
	Lignin microspheres	33.9	Ge *et al*. (2016)
	EAL	8.55	This study
	ECLNPs	125.95	This study
Cu(II)	Polycarboxylic microspheres	1.9	Dakova *et al*. (2009)
	Nanometer-sized ZrO_2	1.3	Dakova *et al*. (2009)
	EAL	9.85	This study
	ECLNPs	54.45	This study

Note: Q_e is the experimental value.

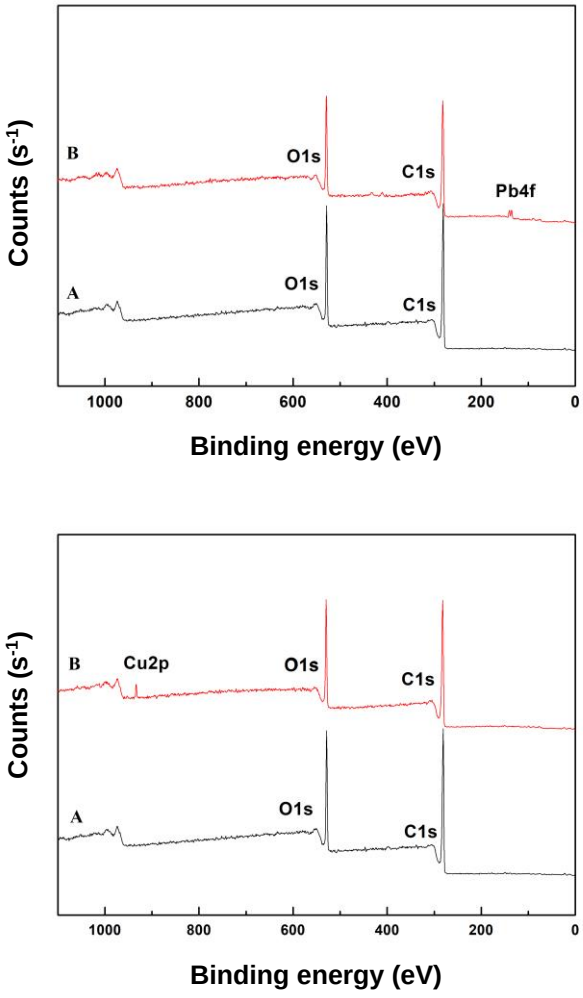

Fig. 3. XPS spectra of EAL and ECLNPs before (A) and after(B) adsorption of Pb(II) and Cu(II)

Isothermal Adsorption Study

The adsorptions of Pb(II) and Cu(II) were conducted under their optimum conditions and the initial concentration of 25, 50, 75, 100, 150, and 200 mg/L (Table 3).

Table 3. Optimum Experimental Conditions of Pb(II) and Cu(II) Adsorption

	pH	Temperature (°C)	Dosage (mg/50 mL)	Time (min)
Pb^{2+}	6.0	30	20	180
Cu^{2+}	5.5	30	20	180

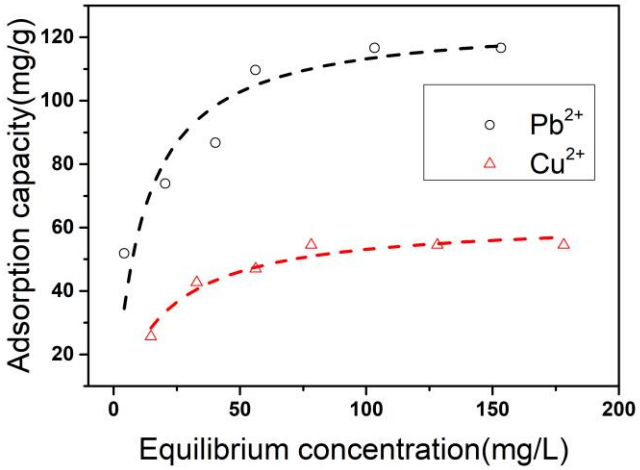

Fig. 4. Langmuir adsorption isotherms of Pb(II) and Cu(II) by ECLNPs

Figure 4 shows the Langmuir adsorption isotherms, representing the relationship between the concentration of heavy metal ions on the ECLNPs and the equilibrium concentration of metal ions in the solution. With the increase of Pb(II) concentration and Cu(II) concentration, the absorbing capacity of ECLNPs to Pb(II) and Cu(II) increased rapidly. When the concentration continued to increase, the adsorption capacity tended to be stable. The Langmuir and Freundlich isotherm models are two commonly used theoretical models to describe adsorption. The Langmuir isothermal model assumes that the adsorption of heavy metal ions is a monolayer adsorption and that the non-interacting adsorption sites have the same adsorption energy (González *et al*. 2015). The Freundlich isothermal model is commonly employed to describe heterogeneous adsorption systems (Brdar *et al*. 2012). Equations 2 and 3 display the Langmuir and Freundlich models, respectively,

$$\frac{C_e}{Q_e} = \frac{C_e}{Q_{max}} + \frac{1}{Q_{max}K_L} \quad (2)$$

$$logQ_e = logK_F + \frac{1}{n}logC_e \quad (3)$$

where C_e (mg/L) is the equalized concentration of metal ions in solution, Q_e (mg/g) is the equalized absorbing quantity of metal ions, Q_{max} (mg/g) is the theoretical saturated absorbing capacity, K_L (L/mg) is a Langmuir constant, and K_F (mg/g)(L/mg)$^{\wedge(1/n)}$ and n are the Freundlich constants.

The fitting curves and parameters are shown in Fig. 5 and Table 4. For Pb(II) adsorption, the adsorptive process fitted well to the Langmuir model (R^2 = 0.9917) rather than the Freundlich model (R^2 = 0.9483), and the calculated saturated absorbing capacity (Q_{max} = 125.9 mg/g) was close to experimental value (116.8 mg/g). As for Cu(II) adsorption, the results were similar to Pb(II) adsorption. Both sets of experimental data fit well with the Langmuir isotherm model, indicating that the two adsorption processes are based on

the monolayer adsorption pattern (Brdar *et al*. 2012). These findings imply that the distribution of adsorption sites on ECLNPs is homogeneous, and this is attributed to the use of the uniform, nanoscale particles. The maximum absorbing capacity of Pb(II) (125.94 mg/g) exceeded that of Cu(II) (60.1 mg/g). The K_L value of ECLNPs to Pb(II) (0.0888 L/mg) was greater than the one of ECLNPs to Cu(II) (0.0674 L/mg), which indicated that the affinity of Pb(II) and ECLNPs was stronger than that of Cu(II) and ECLNPs. Thus, the Pb(II) adsorption process was more efficient.

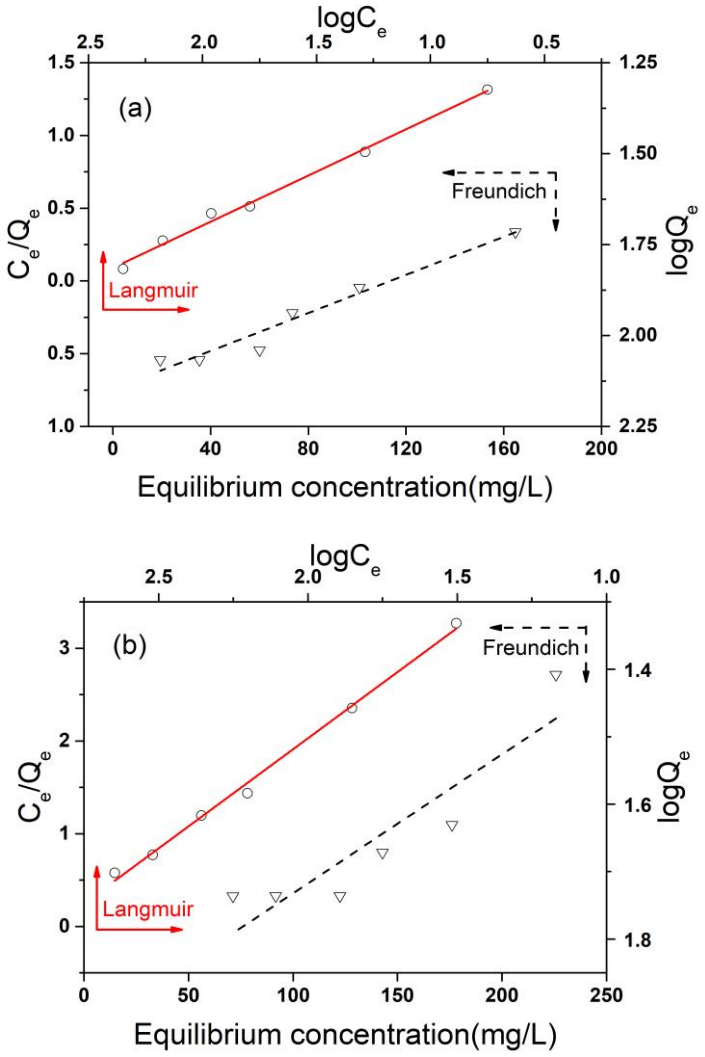

Fig. 5. Fits to the Langmuir and Freundlich isotherm models of Pb(II) (a) and Cu(II) (b) by ECLNPs

Table 4. Isotherm Parameter of ECLNPs with Pb(II) and Cu(II)

	Langmuir		Freundlich	
Pb(II)	K_L/L/mg	0.0888	K_F/mg/g	4.7721
	Q_{max}/mg/g	125.94	*n*	4.09
	R^2	0.99169	R^2	0.94834
Cu(II)	K_L/L/mg	0.0674	K_F/mg/g	3.0920
	Q_{max}/mg/g	60.13	*n*	3.40
	R^2	0.99421	R^2	0.78978

Adsorption Kinetics Study

Adsorption time is a crucial factor for an adsorbent. The effect of contact time is shown in Fig. 2. In Pb(II) and Cu(II) adsorption, the adsorption amount increased sharply from 0 to 30 min, and then it gradually stabilized, reflecting saturation. At the beginning of the reaction, effective active sites were numerous for the combination of metal ions and ECLNPs, resulting in a high adsorption capacity. Gradually the sites on the surface were almost fully occupied. The electrostatic repulsion between ion-loaded ECLNPs and metal ions strengthened as the concentration of ion-loaded ECLNPs increased. Thus, the adsorption rate slowed down (Engil and Zacar 2008).

The pseudo-first-order and pseudo-second-order models (Simonin 2016) were used to investigate the adsorption kinetics. In the pseudo-first-order kinetic reaction, the binding of adsorbates from the solution to the adsorbent surface is mainly affected by diffusion, and there is only one kind of binding site on the adsorbent surface. The pseudo-first-order and pseudo-second-order models are displayed in Eqs. 4 and 5, respectively,

$$\log(Q_e - Q_t) = logQ_e - (\frac{K_1 t}{2.303}) \quad (4)$$

$$\frac{t}{Q_t} = \frac{1}{K_2 Q_e^2} + \frac{t}{Q_e} \quad (5)$$

where Q_t (mg/g) is the absorbing quantity at time t (min), and K_1 (1/min) and K_2 (g/(mg·min)) are rate constants.

The calculated parameters and correlation coefficients of the two models are shown in Table 5. In the pseudo-first-order model of Pb(II) adsorption, the calculated Q_e did not match the experimental one, with a low R^2 value (0.7535). This result indicated that the first-order model cannot account well for the adsorption kinetics. For the pseudo-second-order model, the experimental adsorption amount was close to the calculated value of Q_e (128.2 mg/g), with a higher R^2 value (0.9999), which means the adsorption process accorded with pseudo-second-order kinetics. Cu(II) adsorption showed a similar result. It is noteworthy that the good fit adsorption data to the PSO model likely is due to a diffusion-limited mechanism, based on a review of the literature (Hubbe *et al.* 2019). On the one hand, the metal ions were adsorbed onto ECLNPs through chelation, the reactive steps are relatively rapid and unlikely to be the rate-determining factor. And much typical cases have considered that the rate-limiting step is controlled by the diffusion-based mechanism. On the other hand, the metal ions are positively charged and ECLNPs with -COOH are negatively charged, so the affinity between metal ions and ECLNPs might slow down the progress of diffusion. In addition, the ultimate attachment of metal ions to adsorption sites might be the rate-limiting step. However, the adsorption data in this article are not sufficient to support and verify the either of two assumptions. So more works are needed in the future to confirm the adsorption mechanisms to reveal the rate-limiting process.

Table 5. Adsorption Kinetic Parameters of ECLNPs towards Pb(II) and Cu(II)

		Pseudo-first-order			Pseudo-second-order		
	$Q_{e,exp}$/ mg/g	K_1/min^{-1}	R^2	$Q_{e,cal}$/ mg/g	$Q_{e,cal}$/ mg/g	K_2/g/(mg·min)	R^2
Pb(II)	125.95	0.25193	0.7535	88.22	128.21	0.00268	0.9999
Cu(II)	54.45	0.05041	0.8895	4.19	55.25	0.00767	0.9999

Note: $Q_{e,exp}$ is the experimental value; $Q_{e,cal}$ is the calculated value.

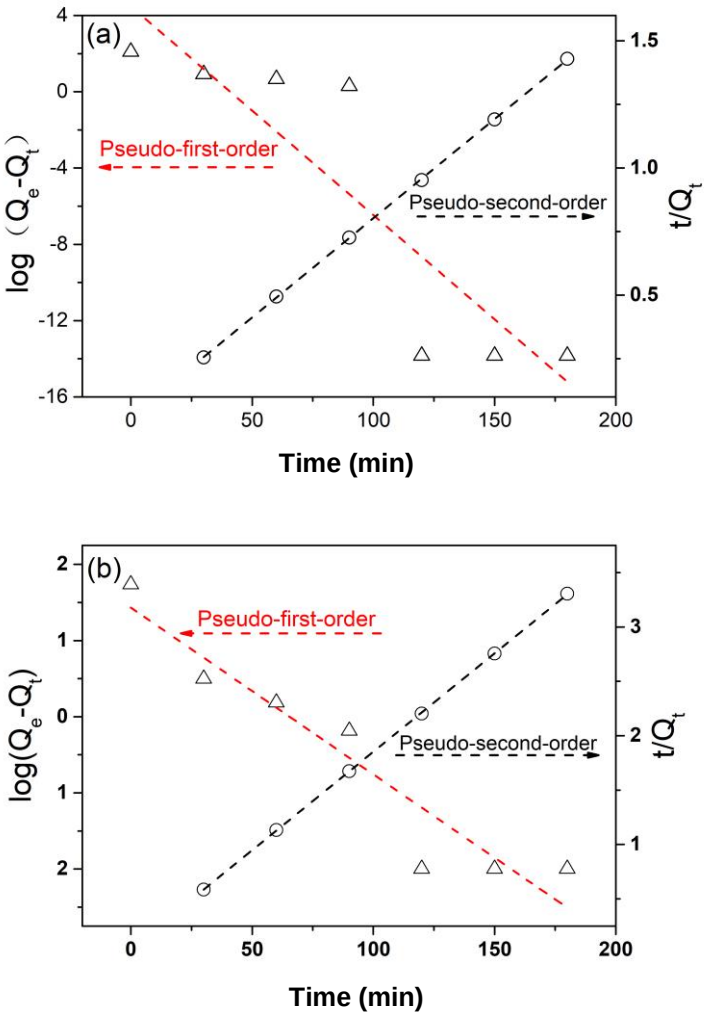

Fig. 6. The Pseudo-first-order and pseudo-second-order kinetic models of Pb(II) (a) and Cu(II) (b)

Comparison Between Pb(II) and Cu(II) Adsorption in Simultaneous Adsorption

To analyze the selectivity of Pb(II) and Cu(II) by ECLNPs, an adsorption study was carried out in mixed solution with the concentration of 100 mg/L by 20 mg ECLNPs at pH 5.75. In Fig. 7, the Pb(II) adsorption quantity increased greatly in the early 15 min, while the Cu(II) adsorption quantity did not, which means that Pb(II) had stronger competitiveness for effective sites of ECLNPs than Cu(II) when the initial concentration was the same. After 15 min, the concentration of Pb(II) decreased and was lower than the concentration of Cu(II), leading to the slighter increase of Pb(II) adsorption capacity and the beginning of Cu(II) adsorption. At 60 min later, both the absorbing capacity of Pb(II) and Cu(II) were constant, resulting from the adsorption saturation of ECLNPs sites. Despite mass amounts differ greatly, the molar amounts for Pb(II) (0.41 mmol/L) and Cu(II) (0.39 mmol/L) are quite similar. It might be the numerical coincidence. In single ion adsorption, the absorbing capacity of Pb(II) and Cu(II) are 0.61 mmol/L and 0.86 mmol/L, respectively. There was a great decease in Cu(II) adsorption capacity than Pb(II), resulting in the weak competitiveness of Cu(II).

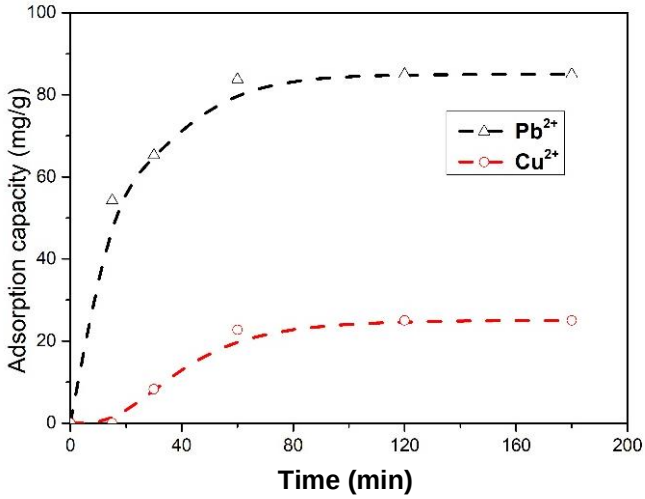

Fig. 7. Simultaneous adsorption kinetics curves of ECLNPs towards Pb(II) and Cu(II)

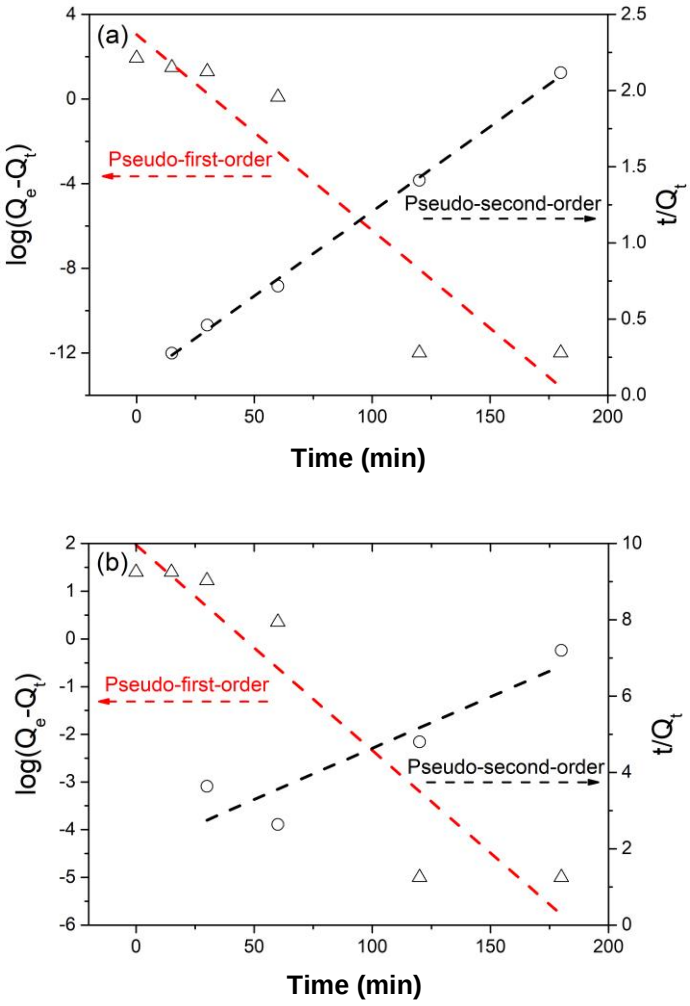

Fig. 8. Pseudo-first-order and pseudo-second-order kinetic models of Pb(II) (a) and Cu(II) (b) in mixed solution

Table 6. Adsorption Kinetic Model Parameters of ECLNPs Towards Pb(II) and Cu(II) in Mixed Solution

		Pseudo-first-order			Pseudo-second-order		
	$Q_{e,exp}$/ mg/g	K_1/min^{-1}	R^2	$Q_{e,cal}$/ mg/g	$Q_{e,cal}$/ mg/g	K_2/g/(mg·min)	R^2
Pb(II)	85.00	0.21309	0.7535	21.0424	90.01	0.00127	0.9976
Cu(II)	25.00	0.09866	0.8895	6.94206	37.12	0.00037	0.7484

Note: $Q_{e,exp}$ is the experimental value, $Q_{e,cal}$ is the calculated value

The kinetic parameters and correlation coefficients of ECLNPs on Pb(II) and Cu(II) in mixed solution are shown in Table 6 and Fig. 8. The Pb(II) adsorption process accorded with pseudo-second-order kinetics (R^2=0.9976), but K_2 (0.00127 g/(mg·min)) in the two-ion solution was smaller than the one (0.00268 g/(mg·min)) in single ion solution. There was an obvious competitive adsorption process between Pb(II) and Cu(II) in solution, which reduced the absorbing amount of Pb(II). The adsorption rate Pb(II) by ECLNPs was smaller. The Cu(II) adsorption followed neither the pseudo-first-order (R^2=0.8895), nor the pseudo-second-order (R^2=0.7484). The presence of Pb(II) inhibited the adsorption of Cu(II), and the adsorption capacity of Cu(II) decreased by nearly 50%. This result suggests that the competitive adsorptive process between two metal ions lowered the adsorption rate, and strong competition from Pb(II) impeded Cu(II) absorption.

The adsorption studies showed that Pb(II) was adsorbed before Cu(II). The absorbed Pb(II) capacity was almost the three times that of absorbed Cu(II). In aqueous solution, metal ions generally exist as hydrated ions. As mentioned above, the molar adsorbing capacity of Cu(II) and Pb(II) is almost similar. The lead atom is much heavier than the copper atom, which can account for its higher mass adsorption capacity. What's more, the affinity of ECLNPs and metal ions related to the valence electron configuration, ion radius, and hydration ion radius. With a larger the effective hydration ion radius, it is more difficult for metal ions to exchange with hydrion (H^+) on a carboxyl group (—COOH). In the adsorption of divalent ions Cu(II) and Pb(II), the effective radius of the hydrated ion (R) and the ionic radius (r) coincided with the empirical formula ($R = r + 0.1335$) (Sverjensky and Sahai 1996); the calculated effective radius of each ion is in Table 7. For Pb(II), its effective hydrated ionic radius was slightly bigger than Cu(II), however, resulting in higher equilibrium adsorption amount, probably because its hydration heat is relatively small so that lead hydrate ions were easier to separate from water ligand and became bare Pb(II) to react with carboxyl groups. Therefore, the adsorption performance depends on the functional groups on the adsorbent and the space structure matching between adsorbents and adsorbates. Future studies should address the mechanism of simultaneous adsorption of a variety of metal ions.

Table 7. Ionic Radius, Effective Hydration Radius and Hydration Heat of Cu(II) and Pb(II)

	Cu(II)	**Pb(II)**
Ionic Radius (Nm)	0.073	0.132
Effective Hydration Radius (Nm)	0.2065	0.2655
Hydration Heat (Kj·Mol^{-1})	2119.3	1500.6

Regeneration Study

A series of three desorption-reabsorption cycles were conducted to investigate the regeneration and recyclability of ECLNPs. The copper-loaded (or lead-loaded) ECLNPs can be regenerated in the acid solution, by adding HNO_3 solution, neutralizing with NaOH, and washing. Figure 9 shows that after three consecutive desorption-reabsorption cycles, there were less losses in Pb(II) and Cu(II) adsorption capacity (Sharma and Mishra 2010), calculated at 16.6% and 21.1%, respectively. ECLNPs have comparatively stable adsorption capacity. The results show that ECLNPs have potential application value as environmentally friendly and low-cost wastewater purification adsorbents.

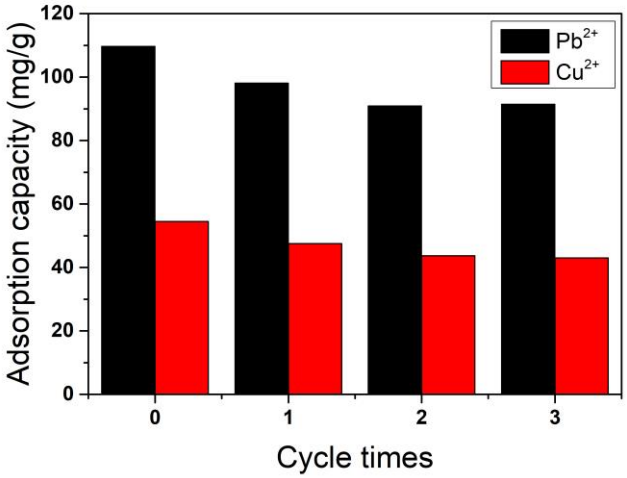

Fig. 9. Pb(II) and Cu(II) adsorption capacity of ECLNPs at different regeneration cycles (ECLNPs dosage =20 mg/50 mL, C_0=100 mg/L, temperature = 30 °C, $pH_{Cu(II)}$ = 5.5, $pH_{Pb(II)}$ = 6.0)

CONCLUSIONS

1. In this work, a new adsorbent made from eucalyptus lignin was synthesized by two simple steps and was used to study the adsorption performance. The ECLNPs have a mean diameter of 50 nm and high content of carboxyl groups (0.66mmol/L), which contributed to higher adsorption capacity of Pb(II) (126.0 mg/g) and Cu(II) (54.4 mg/g) compared to raw eucalyptus lignin.
2. The adsorption kinetics parameters and isothermal model parameters indicated that the adsorption process corresponded with the pseudo-second-order model and the Langmuir model. The simultaneous adsorption study indicated that there was a competitive adsorption process between Pb(II) and Cu(II) and that ECLNPs have higher selectivity towards Pb(II) than Cu(II) due to the lower hydration heat of Pb(II). ECLNPs have good recyclability, the adsorbed ECLNPs can easily be regenerated with high stability for several times.
3. The findings show that ECLNP is a potential adsorbent for its eco-friendliness and good adsorption performance of removing Pb(II) and Cu(II) from wastewater. More attention should be paid to the reaction mechanism under the coexistence of mixed ions in the practical application.

ACKNOWLEDGMENTS

This work was supported by the National Key Research and Development Program of China 278 (Grant No. 2017YFB0307901); the National Natural Science Foundation of China 279 (Grant No. 21476091).

REFERENCES CITED

Aoki, N., Fukushima, K., Kurakata, H., Sakamoto, M., and Furuhata, K. (1999). "6-Deoxy-6-mercaptocellulose and its S-substituted derivatives as sorbents for metal ions," *Reactive and Functional Polymers* 42(3), 223-233. DOI: 10.1016/S1381-5148(98)00076-5

Brdar, M., Takaci, A., and Rakic, D. Z. (2012). "Isotherms for the adsorption of Cu(II) onto lignin: Comparison of linear and non-linear methods," *Hemijska Industrija* 66(4), 497-503. DOI: 10.2298/HEMIND111114003B

Celik, A., and Demirbaş, A. (2005). "Removal of heavy metal ions from aqueous solutions via adsorption onto modified lignin from pulping wastes," *Energy Sources* 27(12), 1167-1177. DOI: 10.1080/00908310490479583

Dakova, I. G., Karadjova, I. B., Georgieva, V. T., and Georgiev, G. S. (2009). "Polycarboxylic microsphere polymer gel for solid phase extraction of trace elements," *Microchimica Acta* 164(1-2), 55-61. DOI: 10.1007/s00604-008-0031-4

Granata, A., and Argyropoulos, D. S. (1995). "2-Chloro-4,4,5,5-tetramethyl-1,3,2-dioxaphospholane, a reagent for the accurate determination of the uncondensed and condensed phenolic moieties in lignins," *Journal of Agricultural and Food Chemistry* 43(6), 1538-1544. DOI: 10.1021/jf00054a023

González, M. A., Pavlovic, I., and Barriga, C. (2015). "Cu(II), Pb(II) and Cd(II) sorption on different layered double hydroxides. A kinetic and thermodynamic study and competing factors," *Chemical Engineering Journal* 269, 221-228. DOI: 10.1016/j.cej.2015.01.094

Ge, Y., Qin, L., and Li, Z. (2016). "Lignin microspheres: An effective and recyclable natural polymer-based adsorbent for lead ion removal," *Materials & Design* 95, 141-147. DOI: 10.1016/j.matdes.2016.01.102

Hubbe, M. A., Azizian, S., and Douven, S. (2019). "Implications of apparent pseudo-second-order adsorption kinetics onto cellulosic materials: A review," *BioResources* 14(3), 7582-7626. DOI: 10.15376/biores.14.3.7582-7626

Liu, C., Li, Y., and Hou, Y. (2018). "Basicity characterization of imidazolyl ionic liquids and their application for biomass dissolution," *International Journal of Chemical Engineering*. DOI: 10.1155/2018/7501659

Liu, C., Li, Y., and Hou Y. (2019). "Preparation of a novel lignin nanosphere adsorbent for enhancing adsorption of lead," *Molecules* 24(15). DOI: 10.3390/molecules24152704

Li, Y., Zhao, R. B., Pang, Y. X., Qiu, X. Q., and Yang, D. J. (2018). "Microwave-assisted synthesis of high carboxyl content of lignin for enhancing adsorption of lead," *Colloids and Surfaces A: Physicochemical and Engineering Aspects* 553, 187-194. DOI: 10.1016/j.colsurfa.2018.05.029

Malek, A., Thomas, T., and Prasad, E. (2016). "Visual and optical sensing of Hg^{2+}, Cd^{2+}, Cu^{2+}, and Pb^{2+} in water and its beneficiation via gettering in nanoamalgam form,"

ACS Sustainable Chemistry & Engineering 4(6), 3497-3503. DOI: 10.1021/acssuschemeng.6b00543

Meena, N. K., Prakasam, M., Bhushan, R., Sarkar, S., Diwate, P., and Banerji, U. (2017). "Last-five-decade heavy metal pollution records from the Rewalsar Lake, Himachal Pradesh, India," *Environ. Earth Sciences* 76(1), 39. DOI: 10.1007/s12665-016-6303-0

Nonkumwong, J., Ananta, S., and Srisombat, L. (2016). "Effective removal of lead(ii) from wastewater by amine-functionalized magnesium ferrite nanoparticles," *RSC Advances* 6(53), 47382-47393. DOI: 10.1039/c6ra07680g

Nguyen, P. H. D., Nguyen, K. T. L., Nguyen, T. T. N., Duong, N. L., Hoang, T. C., Pham, T. T. P., and Vo, D. V. N. (2019). "Application of microwave-assisted technology: A green process to produce ginger products without waste," *Journal of Food Process Engineering* 42(3). DOI: 10.1111/jfpe.12996

Sharma, A. K., and Mishra, A. K. (2010). "Microwave induced β -cyclodextrin modification of chitosan for lead sorption," *International Journal of Biological Macromolecules* 47(3), 410-419. DOI: 10.1016/j.ijbiomac.2010.06.012

Sverjensky, D. A., and Sahai, N. (1996). "Theoretical prediction of single-site surface-protonation equilibrium constants for oxides and silicates in water," *Geochimica et Cosmochimica Acta* 60(20), 3773-3797. DOI: 10.1016/0016-7037(96)00207-4

Simonin, J. (2016). "On the comparison of pseudo-first order and pseudo-second order rate laws in the modeling of adsorption kinetics," *Chemical Engineering Journal* 300, 254-263. DOI: 10.1016/j.cej.2016.04.079

Şengil, İ. A., and Özacar, M. (2008). "Biosorption of Cu(II) from aqueous solutions by mimosa tannin gel," *Journal of Hazardous Materials* 157(2), 277-285. DOI: 10.1016/j.jhazmat.2007.12.115

Wang, H. H., Ni, Y. H., Jahan, M. S., Liu, Z. H., and Schafer, T. (2011). "Stability of cross-linked acetic acid lignin-containing polyurethane," *Journal of Thermal Analysis and Calorimetry* 103(1), 293-302. DOI: 10.1007/s10973-010-1052-x

Yan, M., and Li, Z. (2016). "Microwave-assisted functionalized lignin with dithiocarbamate for enhancing adsorption of Pb(II)," *Materials Letters* 170, 135-138. DOI: 10.1016/j.matlet.2016.02.028

Zhao, X., Zhang, G., Jia, Q., Zhao, C. J., Zhou, W. H., and Li, W. J. (2011). "Adsorption of Cu(II), Pb(II), Co(II), Ni(II), and Cd(II) from aqueous solution by poly(aryl ether ketone) containing pendant carboxyl groups (PEK-L): Equilibrium, kinetics, and thermodynamics," *Chemical Engineering Journal* 171(1), 152-158. DOI: 10.1016/j.cej.2011.03.080

Zong, E. M., Huang, G. B., Liu, X. H., Lei, W. W., Jiang, S. T., Ma, Z. Q., Wang, J. F., and Song, P. G. (2018). "A lignin-based nano-adsorbent for superfast and highly selective removal of phosphate," *Journal of Materials Chemistry A* 6(21), 9971-9983. DOI: 10.1039/c8ta01449c

Article submitted: August 11, 2020; Peer review completed: September 13, 2020; Revised version received: September 18, 2020; Further revised version received: October 4, 2020; Accepted: November 8, 2020; Published: November 13, 2020.
DOI: 10.15376/biores.16.1.249-262